Bioorganic & Medicinal Chemistry 19 (2011) 3474–3482

Contents lists available at ScienceDirect

Bioorganic & Medicinal Chemistry

journal homepage: www.elsevier.com/locate/bmc

Tyrosinase inhibitory activity of a 6-isoprenoid-substituted flavanone isolated from *Dalea elegans*

María Eugenia Chiari [a], Domingo Mariano A. Vera [b], Sara María Palacios [a], María Cecilia Carpinella [a,*]

[a] Fine Chemical and Natural Products Laboratory, School of Chemistry, Catholic University of Córdoba, Camino a Alta Gracia Km 10, (5000) Córdoba, Argentina
[b] Department of Chemistry, School of Exact Sciences, National University of Mar del Plata, Funes esq. Rodriguez-Peña CP 7600, Mar del Plata, Argentina

ARTICLE INFO

Article history:
Received 17 December 2010
Revised 7 April 2011
Accepted 12 April 2011
Available online 16 April 2011

Keywords:
Tyrosinase inhibitors
Dalea elegans
5,2′,4′-Trihydroxy-2″,2″-dimethylchromene-(6,7:5″,6″)-flavanone

ABSTRACT

To aid the pharmaceutical and cosmetic industry in the development of alternatives to prevent melanin-related hyperpigmentation disorders, the plant *Dalea elegans* was submitted to fractionation with the aim of obtaining its anti-tyrosinase principle. Bioguided fractionation of *D. elegans* led to the isolation of 5,2′,4′-trihydroxy-2″,2″-dimethylchromene-(6,7:5″,6″)-flavanone (**1**) as the active compound. This novel flavanone, named as dalenin, showed notable activity at inhibiting tyrosinase using L-tyrosine or L-DOPA as substrates with IC_{50} values of 0.26 and 18.61 μM, respectively. This meant that the flavanone was 52 and 495 times more effective as a monophenolase inhibitor than hydroquinone and kojic acid, respectively. With L-DOPA as a substrate, compound **1** showed itself 59 times more effective at inhibiting the enzyme than hydroquinone and showed the same level of effectiveness as that of kojic acid. It was found that the flavanone behaved as a reversible inhibitor of the enzyme and that it was a mixed-I type or a non-competitive inhibitor with L-tyrosine or L-DOPA as substrates, respectively. Molecular modeling studies were conducted confirming the inhibitory potency of dalenin and showing that the 2′,4′-dihydroxy substituents are important for the interaction with the enzyme.

The results suggest that compound **1** has great potential to be further developed as a pharmaceutical and cosmetic agent for use in dermatological disorders associated with melanin.

1. Introduction

Tyrosinase is a copper-containing enzyme involved in melanogenesis.[1] Also known as polyphenol oxidase (PPO), it is widely distributed in nature and is involved in the first two steps of the melanin biosynthesis[2] in which L-tyrosine is hydroxylated to 3,4-dihydroxyphenylalanine L-DOPA (monophenolase activity) and the latter is subsequently oxidated to dopaquinone (diphenolase activity).[3]

Excessive accumulation of melanin, due to the overexpression of tyrosinase,[4] leads to skin disorders such as age spots, freckles, melasma and malignant melanoma.[5,6] Tyrosinase may also be related to neuromelanin formation[7] and has the potential to produce neurotoxicity by synthesizing dopamine–quinones, which contribute to neurodegeneration associated with Parkinson's disease.[8] Melanin also protects microbes against UV radiation and contributes to microbial virulence.[9] In addition, this pigment has the property of binding to certain antibiotics and antifungals, thus decreasing their effectiveness.[9]

Despite the large number of tyrosinase inhibitors, only a few of these are used today, as many of them show side effects.[10,11] Several compounds, such as the well-known tyrosinase inhibitors, hydroquinone, kojic acid and corticosteroids, can cause adverse reactions such as dermatitis and skin irritation,[12] melanocyte destruction, post-inflammatory pigmentation,[13] ochronosis, cytotoxicity and skin cancer.[10] In this situation, it has been necessary to search for new candidates that show effective tyrosinase inhibition but are devoid of side effects, and metabolites biosynthesized by plants become promising alternatives to the synthetic analogues.[14,15]

In our continuing search for new tyrosinase inhibitors of plant-origin, 91 native plants from central Argentina were screened for their anti-tyrosinase action.[3] From this study, *Dalea elegans* showed the highest inhibition, followed by *Lithrea molleoides*. From this last plant, a highly potent compound identified as (*Z*,*Z*)-5-(trideca-4,7-dienyl)-resorcinol was obtained.[3]

We describe here the isolation of a novel and effective anti-tyrosinase compound obtained from *D. elegans*. The inhibitory

Abbreviations: IC_{50}, the inhibitor concentration leading to 50% activity loss; K_I, inhibition constant; V_{max}, maximum velocity; K_m, Michaelis–Menten constant; *A*, absorbance; PPO, polyphenol oxidase; L-DOPA, 3,4-dihydroxy-L-phenylalanine; TLC, thin layer chromatography; $CHCl_3$, chloroform; ACN, acetonitrile; MeOH, methanol; HPLC, high performance liquid chromatography.

* Corresponding author. Tel.: +54 0351 4938000x611; fax: +54 0351 4938061.
E-mail addresses: ceciliacarpinella@campus1.uccor.edu.ar, cecicarpi@yahoo.com (M.C. Carpinella).

0968-0896/$ - see front matter © 2011 Elsevier Ltd. All rights reserved.
doi:10.1016/j.bmc.2011.04.025

potency, kinetic mechanism, parameters of inhibition and the interaction of this compound with the enzyme were studied in detail.

2. Results

Responding to the urgent need for new agents with inhibitory activity on tyrosinase, a large number of plant species of native flora of central Argentina were screened for anti-tyrosinase activity.[3] From this study, *D. elegans* showed the greatest effectiveness,[3] and so it was subjected to activity-guided purification, yielding a new 6-isoprenoid-substituted flavanone (**1**) as its active principle (Fig. 1).

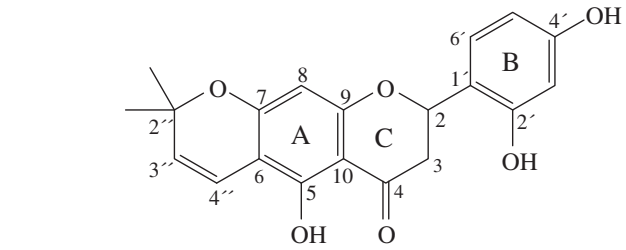

dalenin (**1**)

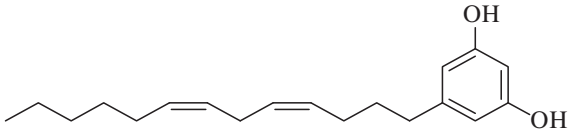

(*Z*,*Z*)-5-(trideca-4, 7-dienyl)-resorcinol (**2**)

Figure 1. Chemical structure of dalenin (**1**) and (*Z*,*Z*)-5-(trideca-4,7-dienyl)-resorcinol (**2**).

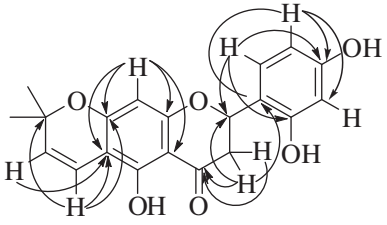

dalenin (**1**)

Figure 2. C/H long-range correlations of **1** obtained from HMBC spectra.

Table 1
Inhibitory effects of dalenin (**1**) on mushroom tyrosinase activity

Compound	Substrate	
	L-Tyrosine IC_{50}[a,b] (μM)	L-DOPA IC_{50}[a,c] (μM)
1	0.26 (0.07, 1.03)	18.61 (7.24, 41.82)
Hydroquinone	13.48 (7.15, 25.44)	1090.56 (287.31, 4139.53)
Kojic acid	128.64 (66.10, 250.33)	18.57 (7.46, 46.24)

[a] IC_{50} values and 95% confidence limits (lower, upper).
[b] Value at 10 min from the beginning.
[c] Value at 2 min from the beginning.

2.1. Identification of the tyrosinase inhibitor obtained from *D. elegans*

According to data obtained in ^{1}H and ^{13}C NMR spectra, a methylene at δ_c 39.9, an oxymethine at δ_c = 76.6, an ABX system at δ_H

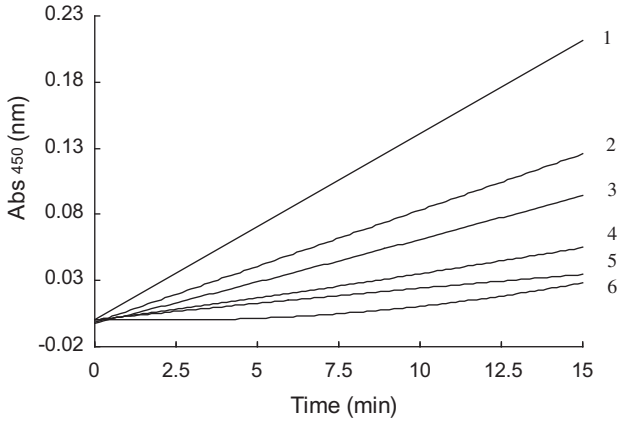

Figure 3. Course of the oxidation of L-tyrosine by tyrosinase in the presence of different concentrations of dalenin (**1**). Concentrations of **1** for curves 1–6 were 0, 0.17, 0.34, 1.37, 2.76 and 5.51 μM, respectively. Compound **1** was incubated with tyrosinase at 37 °C with L-tyrosine as substrate. Dopachrome formation was determined at different times up to 15 min.

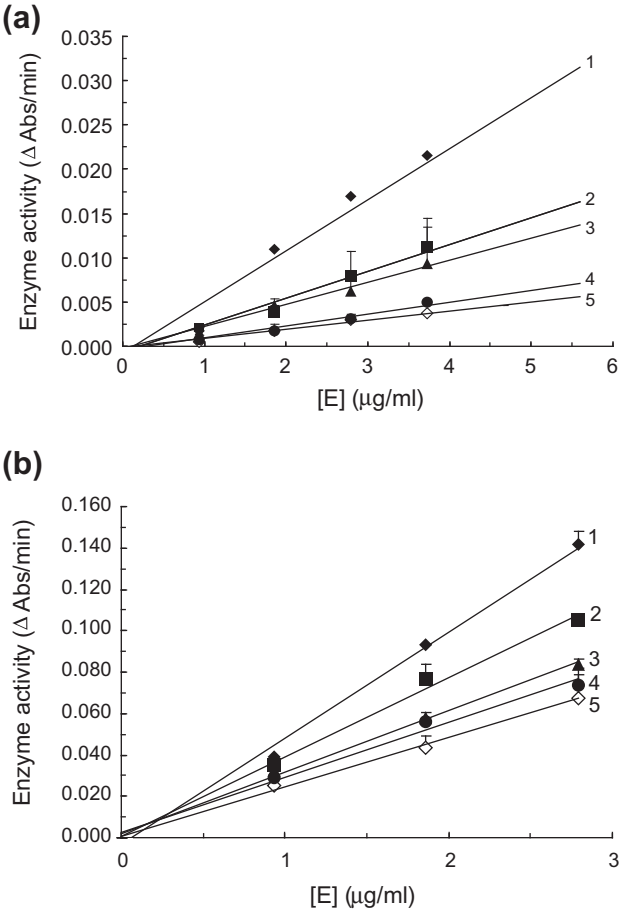

Figure 4. Effects of concentrations of mushroom tyrosinase on its activity for the catalysis of L-tyrosine or L-DOPA at different concentrations of dalenin (**1**). Concentrations of **1** for curves 1–5 were 0, 0.17, 0.34, 0.69 and 1.37 μM, respectively with L-tyrosine as substrate (Fig. 4a) and 0, 11.01, 22.01, 44.02 and 178.35 μM, respectively with L-DOPA as substrate (Fig. 4b). Values are mean ± SD of two separate experiments.

2.88, 3.09 and at δ_H 5.61, assigned to the two H3 and to H2, respectively and a carbonyl group at δ_c = 196.4 were present. These chemical shifts are typically assignable to a flavanone skeleton.[16,17] The presence of a 2,2-dimethylchromene ring with two doublet signals at δ_H = 5.48 and 6.52, assigned to the *ortho*-coupled *cis*-olefinic protons, and another two signals at δ_H 1.43 (s) and 1.44 (s), corresponding to protons of the methyl groups, was confirmed by ^{1}H NMR. The aromatic proton present in ring A gave a single signal δ_H 6.01, as expected for a phloroglucinol ring proton of a flavonoid system.[18] A low-field singlet at δ_H 12.09 indicated an OH attached to C-5, which is hydrogen-bonded to the carbonyl carbon present in ring C. Three aromatic protons resonating at δ_H 6.41–7.18, corresponding to the three aryl protons in the ring B, were also observed. ^{1}H–^{1}H COSY relationships allowed unambiguous assignments for all of these proton chemical shifts and supported the substitution pattern. Further evidence to support the proposed structure was obtained from HSQC, HMBC and ROESY. HSQC spectra were used to assigned carbon resonances to their attached protons. All ^{1}H–^{13}C long-range correlations are shown in Figure 2. Strong long-range correlations were observed for the C-8 proton, to the quaternary carbons C-7 and C-9 at δ_C 162.5 and 163.7, respectively. According to the above correlations, the isolated compound was characterized as a 6,7-isoprenoid substituted flavanone. The quaternary carbons C-6 and C-10 were assigned at 102.3 and 102.8 ppm, respectively, as they were connected to H-8 by ^3J correlations. Further, C-6 showed ^3J and ^2J correlations with H-3″ and H-4″, respectively. The ROESY experiment revealed that the methyl group appearing at δ_H 1.43 is coupled to H-3″ and that the methyl showing a signal at δ_H 1.45 was correlated to both H-8 and H-4″, which is as expected for the proposed structure. The molecular formula of dalenin was confirmed by HRESIMS as a $C_{20}H_{18}O_6$ molecule. On the basis of these spectral analyses the isolated compound was identified as a novel 5,2′,4′-trihydroxy-2″,2″-dimethylchromene-(6,7:5″,6″)-flavanone to which we have given the trivial name dalenin (**1**) (Fig. 1).

2.2. Effects of dalenin on the activity of mushroom tyrosinase

This compound showed a strong tyrosinase inhibition when the enzymatic reaction used L-tyrosine as a substrate, with an IC_{50} value of 0.26 μM (0.094 μg/ml), while 50% inhibition of diphenolase activity was reached at 18.61 μM (6.61 μg/ml) (Table 1).

Monophenolase activity is typically characterized by a lag time, which is the time required for the resting *met* form of tyrosinase to be drawn, via reduction by *o*-diphenols, into the *deoxy* form, which then converts to the active *oxy* form. The kinetic course of the oxidation of L-tyrosine observed with the formation of dopachrome in the presence of different concentrations of dalenin indicated that

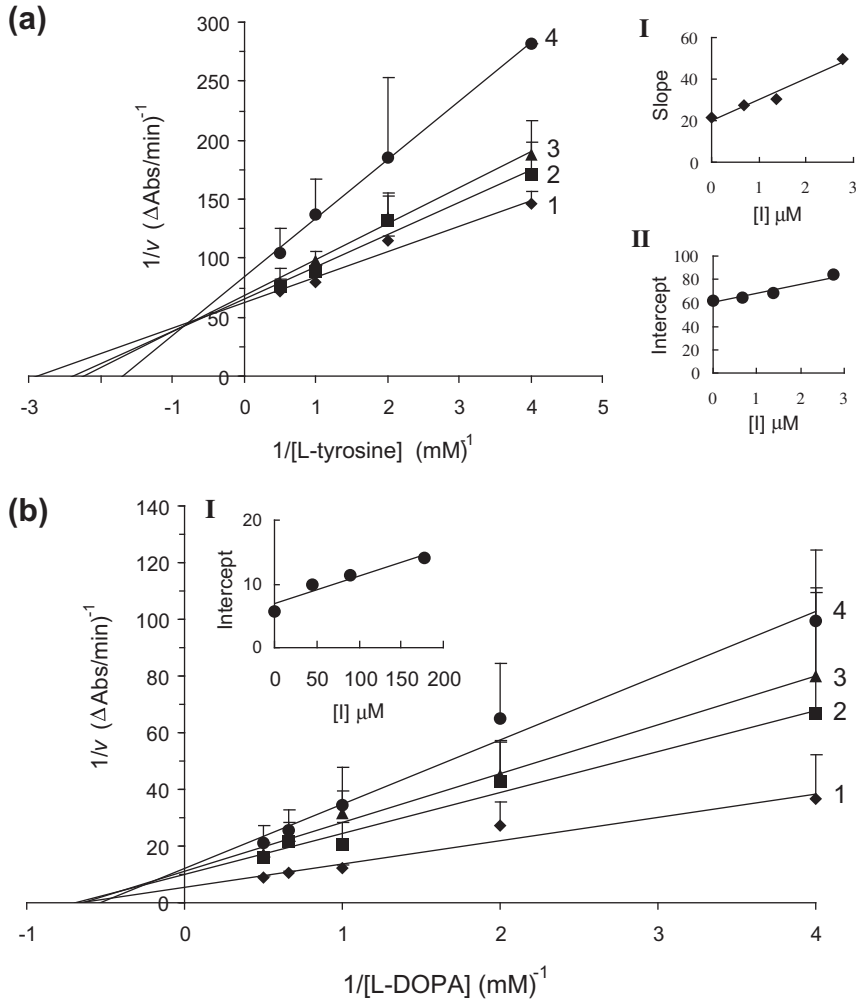

Figure 5. Lineweaver–Burk plots for inhibition of mushroom tyrosinase in presence of dalenin (**1**). Concentrations of **1** for curves 1–4 were 0, 0.69, 1.37 and 2.75 μM, respectively with L-tyrosine as substrate (Fig. 5a) and 0, 44.02, 89.18 and 178.35 μM, respectively with L-DOPA as substrate (b). The insets represent the plot of the slope (aI) or the vertical intercepts ($1/V_{max\ app}$) (aII and bI) versus dalenin concentrations to determine inhibition constants. The lines were drawn using linear least squares fit. Values are mean ± SD of two separate experiments.

the flavanone at 5.51 μM prolonged the lag time to 10 min (Fig. 3). Furthermore, compound **1** reduced the reaction rate in a dose-dependent manner.

2.3. Inhibition of dalenin on tyrosinase using L-tyrosine or L-DOPA as substrates shown to be reversible

The inhibitory mechanism of mushroom tyrosinase by dalenin was studied. The plots of the remaining enzyme activity versus the concentration of enzyme in the presence of different concentrations of dalenin for the catalysis of L-tyrosine and L-DOPA gave a series of straight lines, which all passed through the origin. Increasing the inhibitor concentration resulted in a decrease in the slope of the lines, thus indicating that the enzyme undergoes a reversible inhibition (Fig. 4a and b).

2.4. Inhibition type and inhibition constants of dalenin on tyrosinase using L-tyrosine or L-DOPA as substrates

To obtain further information about the type of inhibition exerted by compound **1**, the kinetic behaviour during the oxidation of L-tyrosine or L-DOPA was analyzed by the Lineweaver–Burk double reciprocal method. The plots for tyrosinase activity in the presence of increasing concentrations of L-tyrosine yield a family of straight lines with different slopes intersecting one another in the second quadrant (Fig. 5a). While the concentration of the flavanone increased, V_{max} decreased and the Michaelis–Menten constant (K_m) increased. These results showed that dalenin was a competitive and uncompetitive mixed-I type inhibitor. When L-DOPA was added as a substrate, increasing concentrations of compound **1** did not modify the K_m of tyrosinase, while they produced a decrease of $V_{max,}$ as observed in the family of lines with different slopes with a common intercept on the *X*-axis (Fig. 5b). This plot indicated that dalenin was a non-competitive inhibitor.

The kinetic parameters of the enzyme for the catalysis of the tested substrates, determined by Lineweaver–Burk plots, are summarized in Table 2.

Table 2
Kinetic parameters of the enzyme for mono- and diphenolase activities with different concentrations of dalenin (**1**)

Kinetic parameters	Substrate	
	L-Tyrosine	L-DOPA
K_m (μM)	346.85	1439.47
V_{max} (ΔAbs/min)	0.0160	0.1754
K_I (μM)	1.98	160.26
K_{IS} (μM)	7.60	160.26

2.5. The chelating ability of dalenin

The bathochromic shifts resulting from complex formation between dalenin and copper ions were investigated. The absorption maximum at 276 nm of dalenin shifted to 286 with the addition of excess Cu^{2+}. With the addition of EDTA, the shifted λ_{max} returned to its original value (276 nm).

2.6. Molecular modeling of the binding of dalenin to tyrosinase

Docking simulations were performed to investigate potential protein–ligand interactions responsible for the great inhibitory activity demonstrated for dalenin in comparison to the well-known inhibitor kojic acid.

Prior to perform the docking simulations, the charge distribution of the active site was characterized by means of DFT[19] (Density Functional Theory) calculations on reduced size models. These first principle calculations were necessary because the

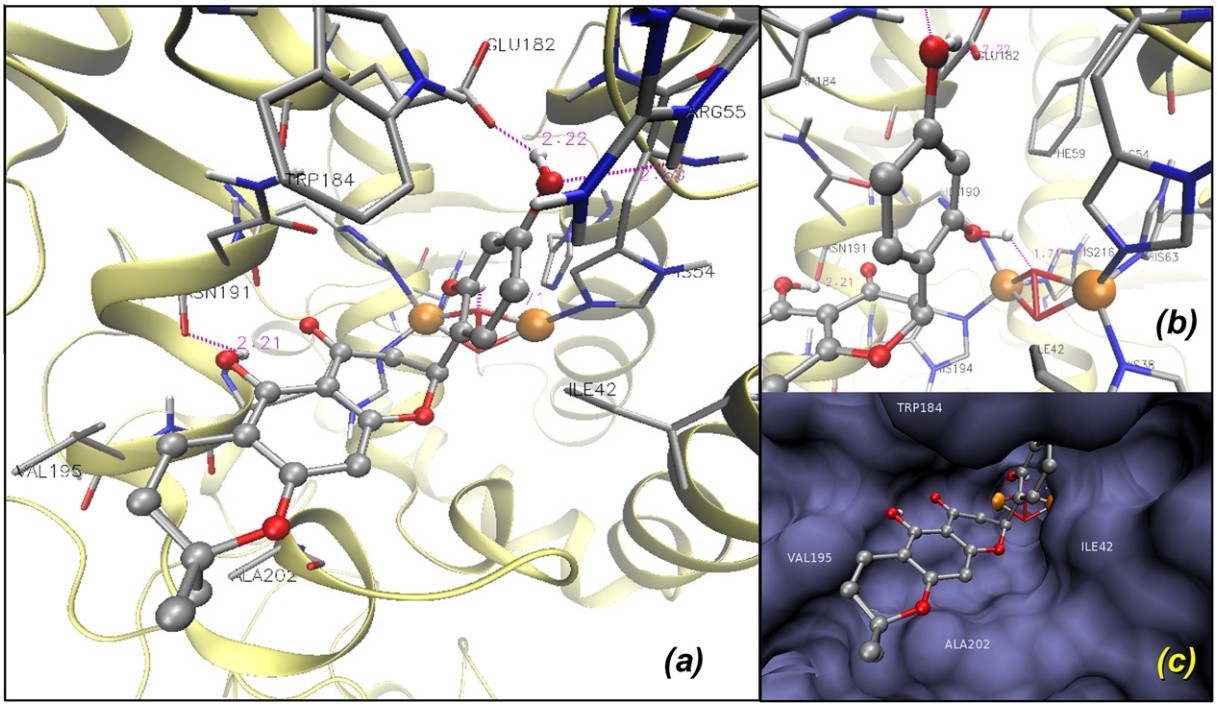

Figure 6. Binding mode of the lowest energy docked conformation found for (2*S*)-dalenin. Cu(II) atoms are shown as golden spheres. The bridging peroxido (O_2) ligand between the metals (red) and the main residues in contact are shown as a licorice representation. The translucent ribbons represent the secondary structure. Hydrogen bonds involving the inhibitor are shown as dotted lines with the bond length (in Å) as labels. Only polar hydrogens of the residues in contact are shown. (a) Overview of the binding of compound **1** (2*S* enantiomer). (b) Zoom of the contacts near the $Cu_2O_2^{2+}$ coordination site. (c) Molecular surface (1.4 Å probe radius) excluding the $Cu_2O_2^{2+}$ complex and the hydrophobic residues in contact to the inhibitor, which feature the entrance to the site.

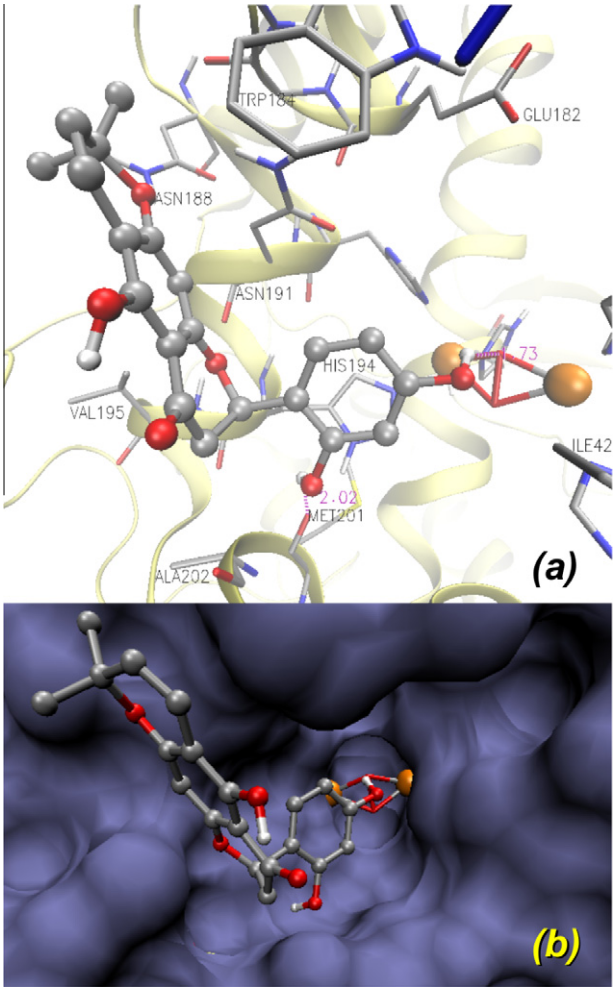

Figure 7. Binding mode of the lowest energy docked conformation found for (2*R*)-dalenin. Cu(II) atoms are shown as golden spheres. The bridging peroxido (O_2) ligand between the metals (red) and the main residues in contact are shown as a licorice representation. The translucent ribbons represent the secondary structure. Hydrogen bonds involving the inhibitor are shown as dotted lines with the bond length (in Å) as labels. Only polar hydrogens of the residues in contact are shown. (a) Overview of the binding of compound **1** (*2S* enantiomer). (b) Molecular surface (1.4 Å probe radius) excluding the $Cu_2O_2^{2+}$ complex and the hydrophobic residues in contact to the inhibitor, which feature the entrance to the site (see also Fig. 6c).

Table 3
Summary of molecular docking results

Compound	Free energy of binding (kcal/mol)	Inhibition constant (K_I) (μM)
(2*S*)-dalenin (**1**)	−6.65	13.8
(2*R*)-dalenin (**1**)	−6.86	9.37
Kojic acid	−4.29	722.2

Estimated free energy of binding and inhibition constants computed for the lowest energy docked structures found for dalenin (**1**) and kojic acid.

electrostatics of a metallo-protein is per se non-trivial and, particularly in the case of the type III copper enzymes, their *oxy* form (the active form which oxidizes L-tyrosine) has a peculiar μ^2-η^2:η^2 bonding involving the couple of copper II ions bridged by a side-on peroxido ligand (Fig. 6a and b).[20–22] The reduced model showed delocalization of the positive formal charge from each Cu^{2+} to the electron rich imidazole rings of the histidines and a localized negative density over the dioxygen bridging ligand facing to the most exposed part of the site (Supplementary data, Fig. S1). This charge pattern, together with the presence of the surrounding charged residues, was found to drive the modes of binding of dalenin.

Since the absolute configuration of the asymmetric C-2 carbon of **1** was not determined, the structures of each enantiomer were optimized and the whole docking protocol was applied separately to both (*2S*)- and (*2R*)-dalenin. Even though there are some examples of (*2R*)-flavanones,[23] most natural occurring flavanones have the *S* configuration in C-2, mainly due to the stereospecificity of the chalcone isomerases and other enzymes involved in their biosynthetic pathways.[24–26] Thus, the discussion will be mainly focused on the *2S* stereoisomer.

The lowest energy binding mode of (*2S*)-dalenin (the lowest cluster of the set of docked conformations) is shown in Figure 6. The 2′,4′ hydroxyl substituents in ring B plays a central role, since this fragment fits well in the metallic enzyme active site. The OH at 2′-position tightly bounds to one of the negative inter-metal oxygens and the 4′-OH is anchored by two H-bonds to the conserved residue Glu182 as donor and to Arg55 as acceptor. In this arrange, the bridging oxygen involved is the one which is most buried in the site. The 5-OH group forms an H-bond with the backbone O of Asn191 (which follows His190 in the sequence, one of the Cu(II) ligands). As shown in Figure 6, several hydrophobic residues feature the shape of the cavity where the three fused rings accommodates themselves. This pose has a binding energy of −6.65 kcal/mol and an estimated K_I of 13.8 μM. A secondary pose was found (the lowest energy conformation of the second cluster), in which the 2′,4′ substitution pattern allows for binding of one hydroxyl group to Glu182 and the other to the bridging O (in this case the O involved is the one most exposed to the entrance to the site, Supplementary data, Fig. S2). The binding energy of this conformation is 0.6 kcal less favored than the one shown in Figure 6.

The lowest energy docked conformation found for the (*2R*) enantiomer has a similar binding energy (−6.86 kcal/mol). For this isomer of dalenin, the 4′-OH bounds the same bridging O as in the case of the *2S* and the 2′-OH is H-bonded to the backbone O of Met201. The 5-OH is solvent exposed and the fused rings arrange into the top branch of the cavity where the fused rings of the *2S* isomer were found (Fig. 7). A secondary pose (0.2 kcal/mol less stable) was found, where both hydroxyl groups of the ring B are comprised in H-bonds involving Glu182 and Arg55, residues which are also involved in the contacts of the ring B of its enantiomer (Supplementary data, Fig. S3). Both enantiomers of dalenin showed substantially most favor binding energies than kojic acid as summarized in Table 3.

3. Discussion

This paper reports the isolation of a novel flavanone, named as dalenin, from the highly effective anti-tyrosinase plant *D. elegans*. This compound, which showed a significant capability to inhibit both oxidative reactions catalysed by tyrosinase (IC_{50} = 0.094 and 6.61 μg/ml for mono- and diphenolase activity of the enzyme, respectively), was 5 and 7 times, respectively, more effective than the starting extract, which showed an IC_{50} of 0.48 and 49.27 μg/ml for both activities of the enzyme, respectively.[3] The presence of synergism between extract components was thus discarded, pointing to dalenin as the only compound responsible for the inhibitory action of the plant.

According to Khatib et al.,[27] those compounds showing IC_{50} values lower than 10 μM are considered as inhibitors with high potency. Dalenin, which showed an IC_{50} of 0.26 μM with the monophenol as substrate (rate-limiting reaction), may therefore be

considered as an excellent candidate to be used as a therapeutic agent for tyrosinase inhibition.

In terms of IC_{50} values (Table 1) and using L-tyrosine as a substrate, dalenin was 52 and 495 times more effective than hydroquinone and kojic acid, respectively, the latter being one of the most powerful anti-tyrosinase agents.[28] Dalenin also showed 6–2108 times more activity than (*Z,Z*)-5-(trideca-4,7-dienil)-resorcinol (**2**) (Fig. 1) (IC_{50} = 1.70 μM),[3] sodium bisulphite (IC_{50} = 210 μM)[29] or arbutin which, depending on the conditions of the assay, showed IC_{50} values of 146 μM[30] or 548 μM.[31]

As observed in Figure 3, dalenin lengthened the lag time. This result confirms the monophenolase inhibition exerted by the isolated compound and is in agreement with the findings obtained with other monophenolase inhibitors such as isoflavones,[32] galangin[33] or glabrene.[34]

When L-DOPA was used as a substrate, dalenin showed itself 59 times more active than hydroquinone and as active as kojic acid (Table 1). The flavanone, in turn, was 3, 7 or 285 times more potent than compound **2** (IC_{50} = 51.87 μM),[3] ascorbic acid (IC_{50} = 140 μM)[35] or arbutin (IC_{50} = 5300 μM),[36] respectively.

As observed in Table 1, dalenin was more effective for inhibiting the first step of oxidation. The fact that the chemical structure of the flavanone resembles more the chemical structure of L-tyrosine with a hydroxyl group at 4-position of the aromatic ring, instead of 3,4-dihydroxy groups as present in L-DOPA, could be the cause for its more potent inhibitory effect in the first stage of activity of the enzyme. These findings are in accordance with those of Kubo et al.[37] and Xie et al.,[38] who observed a higher inhibitory activity on the second activity stage of the enzyme in those compounds showing hydroxyl substituents in 3,4-position than in those presenting 4-hydroxyl. This difference in activity exerted by dalenin matches that obtained for the structurally closed flavanone steppogenin, isolated from *Artocarpus heterophyllus*[30,39] and from *Morus lhou*,[40] which showed higher tyrosinase inhibitory ability when L-tyrosine was used as a substrate (IC_{50} = 1.30 μM) than when L-DOPA was used (IC_{50} = 26.50 μM).[40] The differences in the level of inhibition regarding both activities of tyrosinase were also observed for other compounds, even flavonoids.[34,41]

To ascertain how dalenin behaves, the rate of dopachrome formation was monitored as a function of L-tyrosine concentration. The results obtained by the kinetic analysis indicated that dalenin was a mixed-I type inhibitor, which meant a diminished affinity of the enzyme for the substrate.

The results obtained for diphenolase activity of the enzyme in the presence of different concentrations of dalenin indicated that the inhibitor was able to bind with free enzyme (E) or with enzyme–substrate complex (ES). This non-competitive inhibition may be attributed to the resorcinol subunit present in dalenin, as was reported by Nerya et al.[34] for other anti-tyrosinase compounds.

In view of the inhibitor constant (K_I) values, the interaction between dalenin and tyrosinase exhibited different degrees of affinity when using L-tyrosine or L-DOPA as substrates (K_I = 1.98 and 160.26 μM, respectively, Table 2), with the binding capacity being stronger for the former. These results are logical since dalenin exerted greater inhibitory capacity when L-tyrosine was used as a substrate. The K_I value for dalenin was 15 times lower than that observed for kojic acid (K_I = 30 μM)[42] for monophenolase activity, indicating that the flavanone can bind more tightly to the enzyme than the commercial compound for the hydroxylation of the monophenol. According to our in silico results and besides the limitations of the docking approach, dalenin would be at least 52 times more potent as inhibitor of the *oxy* form of tyrosinase than kojic acid in terms of K_I values (Table 3). This result is in very good agreement with the experimental findings.

On the other hand, the K_I of dalenin for the diphenolase activity of the enzyme was 8 times the value obtained for kojic acid (K_I = 20 μM).[42]

Since K_{IS} was almost four times greater than K_I (see Table 2) for the oxidation of L-tyrosine, dalenin was able to bind more strongly to the free enzyme than to the enzyme–substrate complex.

The potent tyrosinase effectiveness exerted by dalenin may be ascribed to resorcinol substituted ring B, especially with the OH in position 2′,4′. This fact was consistent with the molecular docking results. This substitution pattern was reported as responsible for the anti-tyrosinase activity of many molecules through its binding to the enzyme active site,[27,43] particularly due to OH at 4-position.[44] In fact, substitutions of this OH-group substantially decrease the tyrosinase inhibitory effect of stilbenes and flavanones.[14,40,41] According to Khatib et al.,[43] chalcones with 2,4-dihydroxy substitutions showed themselves more potent than those exhibiting 3,5-dihydroxy derivatives. It should be noted that the potent compound **2**, which exhibits a 3,5 substitution pattern, is a weaker inhibitor than dalenin with 2,4 hydroxyl substituents.

The contacts of the hydroxyl groups of dalenin with one bridging oxygen, Glu182 and Arg55 resemble the contacts of the hydroxyl groups of kojic acid, which showed weaker contacts due to the larger separation between the OH substituents and the lack of the hydrophobic contacts. The lowest energy docked conformation for kojic acid was found to be clearly less stable than for dalenin as summarized in Table 3. The lowest energy conformation of the lowest cluster found in each case are superimposed (Supplementary data, Fig. S4). However, kojic acid has other poses of slightly higher energy (Supplementary data Fig. S5), where its hydroxyl groups are not in contact the Cu_2O_2 moiety.

Besides, dalenin demonstrated chelating ability, which may contribute to enhancing its inhibitory potency.

The free OH functions in ring B are not the only substitution group responsible for the notable activity of dalenin. The presence of the 2,2-dimethylchromene ring system attached at 6–7-position may also be important for the inhibitory effect of dalenin, since the flavanone steppogenin, which presents the same structure as dalenin but lacks the pyrane cycle, is 5 and 1 times less active than dalenin for mono- and diphenolase activity, respectively (see above for IC_{50} values).[40] Besides, it is interesting to note that the chromene cycle not only influences the level of inhibition exerted by both flavanones but also the inhibition mode, since steppogenin behaves as a competitive inhibitor on both oxidative reactions catalyzed by tyrosinase.[40]

The lack of the 2,3-unsaturation pattern seems to make dalenin highly active, since the flavone cycloartocarpesin isolated from *Artocarpus heterophyllus,* and exhibiting the same structure as dalenin but with the abovementioned chemical feature, did not show inhibitory activity of the enzyme with L-tyrosine as substrate at >1000 μM.[39] The same was observed with the flavone cudraflavone B, isolated from the same plant, which presented, in addition to the double bond, an isoprenyl group at 3-position and did not show inhibition even at 23.62 μM.[45]

As reported by Shimizu et al.,[46] those flavanones having 2′,4′-dihydroxy ring B are highly effective monophenolase inhibitors and even better than flavones, flavanonols or flavonols (in descending order of inhibitory activity) with the same ring B structure. This phenomenon matches the notable activity exerted by the flavanone dalenin.

In conclusion, a new 6-isoprenoid flavanone was successfully isolated from *D. elegans*. This compound showed great effectiveness at inhibiting both stages of tyrosinase activity. The new isolated compound studied here has the potential to be further developed as a promising therapeutic agent for treating abnormal skin pigmentation.

4. Materials and methods

4.1. Plant materials

D. elegans Hook. & Arn. (Fabaceae) was collected in the hills of Córdoba Province, Argentina, from November to December 2007–2009. A voucher specimen (UCCOR 254), has been deposited in the 'Marcelino Sayago' Herbarium of the School of Agricultural Science, Catholic University of Córdoba and was authenticated by the botanist, Gustavo Ruiz.

Crushed aerial plant material was extracted by 48 h maceration with 96% ethanol. The yield of extract, obtained after solvent removal and expressed as percentage weight of air-dried crushed plant material, was 11.8 g %.

4.2. Chemicals, equipment and reagents

L-Tyrosine, 3,4-dihydroxy-L-phenylalanine (L-DOPA) and lyophilized mushroom tyrosinase were purchased from Sigma–Aldrich CO (St. Louis, USA). Kojic acid and hydroquinone were obtained from Merck (Darmstadt, Germany). Silica gel (70–230 mesh) used for column chromatography was purchased from Sigma–Aldrich CO and all solvents were HPLC grade. Normal and reversed-phase preparative TLC plates were purchased from Analtech (Newark, DE). ^{1}H and ^{13}CNMR spectra were recorded with a Bruker AVANCE II 400 spectrometer (Bruker Corporation, Ettlingen, Germany). The high resolution MS was determined in a Bruker MicroQTOFII mass spectrometer (Bruker Daltonics, MA, USA), equipped with an ESI source operated in negative mode at 180 °C with a capillary voltage of 4500 V. Mass accuracy was verified by calibration with tunemix. For quantifying the pure compound, HPLC was performed on a Phenomenex Prodigy ODS (4.6 mm i.d. × 250 mm, 5μ) reversed-phase column eluting with 60% methanol in water as a mobile phase and UV detection at 210 nm.

4.3. Isolation of the tyrosinase inhibitor from *D. elegans*

The ethanol extract from *D. elegans* was fractionated using vacuum liquid chromatography on silica gel with $CHCl_3$/ACN gradient to yield nine fractions (Fr_{A1}–Fr_{A9}). Those fractions showing more than 90% inhibition at 10 μg/ml using L-tyrosine as a substrate (Fr_{A3}–Fr_{A4}) were further purified in a column chromatography with the same solvent mixture at increasing polarity, to obtain seven fractions (Fr_{B1}–Fr_{B7}). Of these, Fr_{B4}–Fr_{B5} eluted with $CHCl_3$/ACN 90:10–80:20 showed effectiveness (>90% inhibition at 2.5 μg/ml) and were therefore subjected to radial preparative chromatography. From this process, effective fractions (Fr_{C4}–Fr_{C6}) eluted with hexane/diethyl ether 60:40, were submitted to normal and then reversed-phase preparative TLC plates (MeOH/H_2O 60:40) affording the compound as a yellow powder (yield 0.039 g/100 g of crushed plant material, by HPLC).

This compound was identified as a new 2′,4′-dihydroxyflavanone showing a 2, 2-dimethylchromene ring attached at position 6,7 which was named dalenin (**1**) (Fig. 1).

Dalenin (**1**): t_R 46.8 min (by HPLC). $[\alpha]_D^{26}$ 1.43 (*c* 0.14 in CH_2Cl_2). ^{1}H NMR (400 MHz, $CDCl_3$, 25 °C, TMS): δ 12.09 (1H, s, OH-5), 7.18 (1H, d, *J* = 8.4 Hz, H-6′), 6.52 (1H, d, *J* = 10.2 Hz, H-4″), 6.44 (1H, d, *J* = 8.4 Hz, H-5′), 6.41 (1H, br s, H-3′), 6.01 (1H, s, H-8), 5.61 (1H, dd, *J* = 12.8, 2.8 Hz, H-2), 5.48 (1H, d, *J* = 10.2 Hz, H-3″), 3.09 (1H, dd, *J* = 17.2, 13.0 Hz, H-3), 2.88 (1H, dd, *J* = 17.2, 2.8 Hz, H-3), 1.45 (3H, s, CH_3-2″a), 1.43 (3H, s, CH_3-2″b).^{13}C NMR (100 MHz, $CDCl_3$, 25 °C, TMS): δ = 28.4 CH_3-2″); 28.4 CH_3-2″); 39.9 C-3); 76.6 C-2); 78.4 C-2″); 97.9 C-8); 102.3 C-6); 102.8 C-10); 102.8 C-3′); 107.8 C-5′); 113.9 C-4″); 116.9 C-1′); 124.9 C-3″); 126.9 C-6′); 147.9 C-5); 154.9 C-2′); 157.1 C-4′); 162.5 C-7); 163.7 C-9); 196.4 ppm C-4); UV–vis (ethanol): λ_{max} (ε = 290 (14362), 276 (15750), 206 nm (34164); HR-TOF-MS (ESI negative) *m*/*z*: $[M-H]^-$ calcd for $C_{20}H_{17}O_6$, 353.1031; found, 353.1044.

4.4. Tyrosinase inhibitory assay

Tyrosinase inhibitory activity was determined spectrophotometrically.[3] First, 2 μl of mushroom tyrosinase (2500 U/ml in 50 mM phosphate buffer, pH 6.5) was mixed with 148 μl of 50 mM phosphate buffer. Then, 10 μl of the tested fractions or of the isolated compound previously dissolved in ethanol at the concentrations needed, or of ethanol (control), were added. Finally, 40 μl of 2.5 mM L-tyrosine or L-DOPA in phosphate buffer was added and absorbance was immediately monitored (t = 0) at 450 nm. The assay mixture was then incubated at 37 °C for 15 min, or at ambient temperature for 5 min, with gentle agitation, when L-tyrosine or L-DOPA were used, respectively, in order to monitor dopachrome formation. Kojic acid or hydroquinone, dissolved in 50 mM phosphate buffer, were used as a positive controls.

Differences in absorbance between each time measured and time zero were calculated and the inhibition percentage was determined respect to control. The concentration necessary for 50% inhibition (IC_{50}) was determined. Each measurement was made at least in duplicate.

The inhibition kinetics of the enzyme by the isolated compound was analyzed by the Lineweaver–Burk plots compared to data obtained in the absence of inhibitor (control). Experiments were carried out using the same protocol described above, except for varying concentrations of L-tyrosine or L-DOPA. The inhibition constants for inhibitor binding with free or enzyme–substrate complex, K_I or K_{IS}, respectively with L-tyrosine as substrate, were obtained from the second plots of the slopes of the straight lines or vertical intercept ($1/V_{max}^{app}$), respectively, versus the concentration of dalenin. K_I or K_{IS} and are represented by the Eqs. 1 and 2, respectively:

$$\text{Slope} = \frac{K_m}{K_I V_{max}}[I] + \frac{K_m}{V_{max}} \quad (1)$$

$$\text{Intercept} = \frac{1}{K_{IS} V_{max}}[I] + \frac{1}{V_{max}} \quad (2)$$

With regard to the diphenolase activity of the enzyme, K_I and K_{IS} are the same in quantity and can be obtained from the secondary plot of the intercept on the *Y*-axis versus the inhibitor concentration. K_I may be calculated from Eq. 3.

$$\text{Intercept} = \frac{1}{K_I V_{max}}[I] + \frac{1}{V_{max}} \quad (3)$$

4.5. Chelating ability of the tyrosinase inhibitor from *D. elegans*

To check the chelation of the isolated compound by Cu^{2+}, UV–vis (220–600 nm) spectroscopy was carried out. The compound dissolved in ethanol (84.66 μM) was scanned with aqueous solution of $CuSO_4$ (200 μM) or water (control). A third spectrum after the addition of EDTA (250 μM) was recorded. The resulting spectra were then compared.

4.6. Molecular docking simulations of dalenin and a known inhibitor

Since the novel flavanone dalenin exhibited a remarkable activity as monophenolase inhibitor, it was docked into the *oxy* form of tyrosinase. As in other recent studies,[47–49] the structure of the *oxy* tyrosinase obtained from *Streptomyces castaneoglobisporus* was used as the initial structure for docking simulations after removal

of the caddie protein, the exogenous ions and water molecules (pdb entry 1WX2).[50] In order to address the actual charge distribution of the coordination site, first principles Quantum Mechanics calculations were done at the B3LYP/6-31+G*[51,52] level of theory on reduced models of the site including: the two copper ions, the bridging dioxygen as well as the six imidazoles mimicking the histidines coordinated to the Cu(II) ions. The RESP[53] charges were obtained from the Quantum results and the solvation parameters for copper were similar to those used in Takahashi et al., 2010.[47] For the rest of the protein and for all inhibitors docked, two charge schemes were used: Gasteiger charges (AUTODOCK 4.2 program default)[54,55] and AMBER RESP[53] charges. Only the former set will be discussed, since it is expected to better reproduce experimental inhibition constants, and both binding modes obtained and the relative order of energies were very similar.

The structures of the most stable conformers of the inhibitors were obtained by full geometry optimization, using the same level of theory as for the calculations of the coordination site of the enzyme. The nature of minimum of the stationary points was established by means of the harmonic frequencies analysis, using the GAUSSIAN 03 package.[56] The AUTODOCK 4.2 package[54,55] was used for the docking simulations, precomputing a grid inside a box of $26 \times 24 \times 20$ Å^3, roughly centered at the dioxygen ligand, with a grid spacing of 0.2 Å. For each inhibitor, 2000 runs of a Lamarckian genetic algorithm[54,55] were done, each of them with a population of 150 individuals, up to 100,000 generations, with 1 survivor per generation, a limit of 5×10^6 energy evaluations and the remainder algorithm control parameters set to program defaults. The standard AUTODOCK 4.2 estimation of inhibition constants and free energy of binding are informed after performing a cluster analysis with a 0.5 kcal/mol and 2.0 Å as criteria for energy and RMS, respectively. The analysis and visualization of results were done using MGLTools[54,55] and VMD 1.8.7.[57,58]

4.7. Statistical analysis

The results are expressed as mean ± SD. The inhibitory concentration (IC_{50}) was calculated by log-Probit analysis.

5. Conflict of interest statement

The authors have declared no conflicts of interest.

Acknowledgments

This work was supported by the Catholic University of Córdoba, FONCyT PICT 2005, PICTO CRUP 2005 and FONCYT PICT-PRH #20 2009. We thank Joss Heywood for revising the English language.

Supplementary data

Supplementary data associated with this article can be found, in the online version, at doi:10.1016/j.bmc.2011.04.025.

References and notes

1. Bao, K.; Dai, Y.; Zhu, Z.-B.; Tu, F.-J.; Zhang, W.-G.; Yao, X.-S. *Bioorg. Med. Chem.* **2010**, *18*, 6708.
2. Ghani, U.; Ullah, N. *Bioorg. Med. Chem.* **2010**, *18*, 4042.
3. Chiari, M. E.; Joray, M. B.; Ruiz, G.; Palacios, S. M.; Carpinella, M. C. *Food Chem.* **2010**, *120*, 10.
4. Khan, M. *Top. Heterocycl. Chem.* **2007**, *9*, 119.
5. Chen, Q.-X.; Kubo, I. *J. Agric. Food Chem.* **2002**, *50*, 4108.
6. Prezioso, J. A.; Epperly, M. W.; Wang, N.; Bloomer, W. D. *Cancer Lett.* **1992**, *63*, 73.
7. Xu, Y.; Stokes, A. H.; Freeman, W. M.; Kumer, S. C.; Vogt, B. A.; Vrana, K. E. *Mol. Brain Res.* **1997**, *45*, 159.
8. Greggio, E.; Bergantino, E.; Carter, D.; Ahmad, R.; Costin, G.-E.; Hearing, V. J.; Clarimon, J.; Singleton, A.; Eerola, J.; Hellström, O.; Tienari, P. J.; Miller, D. W.; Beilina, A.; Bubacco, L.; Cookson, M. R. *J. Neurochem.* **2005**, *93*, 246.
9. Nosanchuk, J. D.; Casadevall, A. *Antimicrob. Agents Chemother.* **2006**, *50*, 3519.
10. Karioti, A.; Protopappa, A.; Megoulas, N.; Skaltsa, H. *Bioorg. Med. Chem.* **2007**, *15*, 2708.
11. Okombi, S.; Rival, D.; Bonnet, S.; Mariotte, A.-M.; Perrier, E.; Boumendjel, A. *Bioorg. Med. Chem. Lett.* **2006**, *16*, 2252.
12. Tocco, G.; Fais, A.; Meli, G.; Begala, M.; Podda, G.; Fadda, M. B.; Corda, M.; Attanasi, O. A.; Filippone, P.; Berretta, S. *Bioorg. Med. Chem. Lett.* **2009**, *19*, 36.
13. Chawla, S.; DeLong, M. A.; Visscher, M. O.; Wickett, R. R.; Manga, P.; Boissy, R. E. *Br. J. Dermatol.* **2008**, *159*, 1267.
14. Zheng, Z.-P.; Cheng, K.-W.; Zhu, Q.; Wang, X.-C.; Lin, Z.-X.; Wang, M. *J. Agric. Food Chem.* **2010**, *58*, 5368.
15. Sirat, H. M.; Rezali, M. F.; Ujang, Z. *J. Agric. Food Chem.* **2010**, *58*, 10404.
16. Liu, D.; Lan, R.; Xin, X. L.; Wang, X. J.; Su, D. H.; Yang, G. W. *Chin. Chem. Lett.* **2008**, *19*, 1453.
17. Shi, Y.-Q.; Fukai, T.; Sakagami, H.; Chang, W.-J.; Yang, P.-Q.; Wang, F.-P.; Nomura, T. *J. Nat. Prod.* **2001**, *64*, 181.
18. Nomura, T.; Fukai, T.; Yamada, S.; Katayanagi, M. *Chem. Pharm. Bull.* **1978**, *26*, 1394.
19. Parr, R. G.; Yang, W. *Annu. Rev. Phys. Chem.* **1995**, *46*, 701.
20. Sabolović, J.; Gomzi, V. *J. Chem. Theory Comput.* **2009**, *5*, 1940.
21. Piquemal, J. P.; Pilmé, J.; Parisel, O.; Gérard, H.; Fourré, I.; Bergès, J.; Gourlaouen, C.; De La Lande, A.; Van Severen, M. C.; Silvi, B. *Int. J. Quantum Chem.* **2008**, *108*, 1951.
22. Decker, H.; Tuczek, F. *Trends Biochem. Sci.* **2000**, *25*, 392.
23. Welford, R. W. D.; Clifton, I. J.; Turnbull, J. J.; Wilson, S. C.; Schofield, C. J. *Org. Biomol. Chem.* **2005**, *3*, 3117.
24. Grotewold, E. *The Science of Flavonoids*; New York: Springer, 2008.
25. Stafford, H. A. *Plant Physiol.* **1991**, *96*, 680.
26. Su, B.-N.; Jung Park, E.; Vigo, J. S.; Graham, J. G.; Cabieses, F.; Fong, H. H. S.; Pezzuto, J. M.; Kinghorn, A. D. *Phytochemistry* **2003**, *63*, 335.
27. Khatib, S.; Nerya, O.; Musa, R.; Tamir, S.; Peter, T.; Vaya, J. *J. Med. Chem.* **2007**, *50*, 2676.
28. Jimenez, M.; Garcia-Carmona, F. *J. Agric. Food Chem.* **1997**, *45*, 2061.
29. Friedman, M.; Bautista, F. F. *J. Agric. Food Chem.* **1995**, *43*, 69.
30. Zheng, Z.-P.; Cheng, K.-W.; Chao, J.; Wu, J.; Wang, M. *Food Chem.* **2008**, *106*, 529.
31. Momtaz, S.; Mapunya, B. M.; Houghton, P. J.; Edgerly, C.; Hussein, A.; Naidoo, S.; Lall, N. *J. Ethnopharmacol.* **2008**, *119*, 507.
32. Chang, T.-S.; Ding, H.-Y.; Tai, S. S.-K.; Wu, C.-Y. *Food Chem.* **2007**, *105*, 1430.
33. Kubo, I.; Kinst-Hori, I. *J. Agric. Food Chem.* **1999**, *47*, 4121.
34. Nerya, O.; Vaya, J.; Musa, R.; Izrael, S.; Ben-Arie, R.; Tamir, S. *J. Agric. Food Chem.* **2003**, *51*, 1201.
35. Yi, W.; Wu, X.; Cao, R.; Song, H.; Ma, L. *Food Chem.* **2009**, *117*, 381.
36. Qiu, L.; Chen, Q.-H.; Zhuang, J.-X.; Zhong, X.; Zhou, J.-J.; Guo, Y.-J.; Chen, Q.-X. *Food Chem.* **2009**, *112*, 609.
37. Kubo, I.; Kinst-Hori, I.; Chaudhuri, S. K.; Kubo, Y.; Sánchez, Y.; Ogura, T. *Bioorg. Med. Chem.* **2000**, *8*, 1749.
38. Xie, L. P.; Chen, Q. X.; Huang, H.; Wang, H. Z.; Zhang, R. Q. *Biochemistry (Moscow)* **2003**, *68*, 487.
39. Zheng, Z. P.; Cheng, K. W.; To, J. T. K.; Li, H.; Wang, M. *Mol. Nutr. Food Res.* **2008**, *52*, 1530.
40. Jeong, S. H.; Ryu, Y. B.; Curtis-Long, M. J.; Ryu, H. W.; Baek, Y. S.; Kang, J. E.; Lee, W. S.; Park, K. H. *J. Agric. Food Chem.* **2009**, *57*, 1195.
41. Fu, B.; Li, H.; Wang, X.; Lee, F. S. C.; Cui, S. *J. Agric. Food Chem.* **2005**, *53*, 7408.
42. Chen, J. S.; Wei, C.-i.; Rolle, R. S.; Otwell, W. S.; Balaban, M. O.; Marshall, M. R. *J. Agric. Food Chem.* **1991**, *39*, 1396.
43. Khatib, S.; Nerya, O.; Musa, R.; Shmuel, M.; Tamir, S.; Vaya, J. *Bioorg. Med. Chem.* **2005**, *13*, 433.
44. Nerya, O.; Musa, R.; Khatib, S.; Tamir, S.; Vaya, J. *Phytochemistry* **2004**, *65*, 1389.
45. Zheng, Z.-P.; Chen, S.; Wang, S.; Wang, X.-C.; Cheng, K.-W.; Wu, J.-J.; Yang, D.; Wang, M. *J. Agric. Food Chem.* **2009**, *57*, 6649.
46. Shimizu, K.; Kondo, R.; Sakai, K. *Planta Med.* **2000**, *66*, 11.
47. Takahashi, S.; Kamiya, T.; Saeki, K.; Nezu, T.; Takeuchi, S.-i.; Takasawa, R.; Sunaga, S.; Yoshimori, A.; Ebizuka, S.; Abe, T.; Tanuma, S.-i. *Bioorg. Med. Chem.* **2010**, *18*, 8112.
48. Xue, C.-B.; Zhang, L.; Luo, W.-C.; Xie, X.-Y.; Jiang, L.; Xiao, T. *Bioorg. Med. Chem.* **2007**, *15*, 2006.
49. Deeth, R.; Diedrich, C. *J. Biol. Inorg. Chem.* **2010**, *15*, 117.
50. Matoba, Y.; Kumagai, T.; Yamamoto, A.; Yoshitsu, H.; Sugiyama, M. *J. Biol. Chem.* **2006**, *281*, 8981.
51. Becke, A. D. *J. Chem. Phys.* **1993**, *98*, 5648.
52. Lee, C.; Yang, W.; Parr, R. G. *Phys. Rev. B* **1988**, *37*, 785.
53. Bayly, C. I.; Cieplak, P.; Cornell, W.; Kollman, P. A. *J. Phys. Chem.* **1993**, *97*, 10269.
54. Morris, G. M.; Goodsell, D. S.; Halliday, R. S.; Huey, R.; Hart, W. E.; Belew, R. K.; Olson, A. J. *J. Comput. Chem.* **1998**, *19*, 1639.
55. Autodock 4.2: Morris, G. M.; Pique, M.; Hart, W. E.; Halliday, R. S.; Chang, M.; Gillet, A.; Forli, S.; Belew, R. K.; Goodsell, D. S.; Olson, A. J.. Copyright 1989-2009. The Scripps Research Institute. Autodock Tools 1.5.4: Sanner, M. F.; Huey, R.; Dallakyan, S.; Karnati, S.; Lindstrom, W.; Morris, G. M.; Norledge, B.; Omelchenko, A.; Stoffler, D.; Vareille, G.. Copyright 1999–2009. Molecular Graphics Laboratory, The Scripps Research Institute.
56. Frisch, M. J.; Trucks, G. W.; Schlegel, H. B.; Scuseria, G. E.; Robb, M. A.; Cheeseman, J. R.; Montgomery, J. A.; Vreven, T., Jr.; Kudin, K. N.; Burant, J. C.;

Millam, J. M.; Iyengar, S. S.; Tomasi, J.; Barone, V.; Mennucci, B.; Cossi, M.; Scalmani, G.; Rega, N.; Petersson, G. A.; Nakatsuji, H.; Hada, M.; Ehara, M.; Toyota, K.; Fukuda, R.; Hasegawa, J.; Ishida, M.; Nakajima, T.; Honda, Y.; Kitao, O.; Nakai, H.; Klene, M.; Li, X.; Knox, J. E.; Hratchian, H. P.; Cross, J. B.; Adamo, C.; Jaramillo, J.; Gomperts, R.; Stratmann, R. E.; Yazyev, O.; Austin, A. J.; Cammi, R.; Pomelli, C.; Ochterski, J. W.; Ayala, P. Y.; Morokuma, K.; Voth, G. A.; Salvador, P.; Dannenberg, J. J.; Zakrzewski, V. G.; Dapprich, S.; Daniels, A. D.; Strain, M. C.; Farkas, O.; Malick, D. K.; Rabuck, A. D.; Raghavachari, K.; Foresman, J. B.; Ortiz, J. V.; Cui, Q.; Baboul, A. G.; Clifford, S.; Cioslowski, J.; Stefanov, B. B.; Liu, G.; Liashenko, A.; Piskorz, P.; Komaromi, I.; Martin, R. L.; Fox, D. J.; Keith, T.; Al-Laham, M. A.; Peng, C. Y.; Nanayakkara, A.; Challacombe, M.; Gill, P. M. W.; Johnson, B.; Chen, W.; Wong, M. W.; Gonzalez, C.; Pople, J. A. Gaussian, Inc.: Pittsburgh PA, 2003.

57. Humphrey, W.; Dalke, A.; Schulten, K. *J. Mol. Graphics* **1996**, *14*, 33.
58. Visual Molecular Dynamics VMD 1.8.7. Copyright 2009 University of Illinois at Urbana-Champaign. http://www.ks.uiuc.edu/Research/vmd/.